Lawrence Berkeley National Laboratory

Title

Binary pseudo-random grating as a standard test surface for measurement of modulation transfer function of interferometric microscopes

Permalink

https://escholarship.org/uc/item/1056t8s7

Authors

Yashchuk, Valeriy V.
McKinney, Wayne R.
Takacs, Peter Z.

Publication Date

2007-07-25

Binary pseudo-random grating as a standard test surface for measurement of modulation transfer function of interferometric microscopes

Valeriy V. Yashchuk,*[a] Wayne R. McKinney,[a] and Peter Z. Takacs[b]
[a]Lawrence Berkeley National Laboratory, Berkeley, California, USA, 94720
[b]Brookhaven National Laboratory, Upton, New York, USA, 11973

ABSTRACT

The task of designing high performance X-ray optical systems requires the development of sophisticated X-ray scattering calculations based on rigorous information about the optics. One of the most insightful approaches to these calculations is based on the power spectral density (PSD) distribution of the surface height. The major problem of measurement of a PSD distribution with an interferometric and/or atomic force microscope arises due to the unknown Modulation Transfer Function (MTF) of the instruments. The MTF characterizes the perturbation of the PSD distribution at higher spatial frequencies. Here, we describe a new method and dedicated test surfaces for calibration of the MTF of a microscope. The method is based on use of a specially designed Binary Pseudo-random (BPR) grating. Comparison of a theoretically calculated PSD spectrum of a BPR grating with a spectrum measured with the grating provides the desired calibration of the instrumental MTF. The theoretical background of the method, as well as results of experimental investigations are presented.

Keywords: standard test surface, interferometric microscope, modulation transfer function, power spectral density, optical metrology, calibration, error reduction

1. INTRODUCTION

Surface profilometers, such as interferometric microscopes, have become a basic metrology tool for the characterization of high quality optical surfaces with sub-Angstrom rms roughness. For the last few decades, the standard list of output parameters of an interferometric microscope measurement included values of roughness averaged over an area and along a sample line. This was extended to a more rigorous statistical description of the surface topography based on power spectral density (PSD) distributions of the surface height (see e.g.,[1-4] and references therein). For example, the measured PSD distributions provide a basis for sophisticated calculations of three-dimensional scattering of x-rays by the optics.[5-7]

A straightforward transformation of the measured 2D area distribution of the residual surface heights into a 2D PSD distribution always provides spectra with distortion caused by the unknown spatial frequency response of the instrument. The response is characterized by the modulation transfer function (MTF), determining the bandwidth of the instrument.[8] The MTF contains contributions from the instrumental optical system, detector, signal processing, software algorithm, and environmental factors. Generally, these contributions are difficult to account for separately. The instrumental MTF can be evaluated by comparing a PSD distribution measured using a known test surface with a corresponding ideal numerically simulated PSD.[9-11] The square root of the ratio of the measured and simulated PSD distributions gives the MTF of the instrument. The Binary Pseudo-random (BPR) grating described here provides an effective test surface to fulfill this calibration need.

2. MATHEMATICAL BACKGROUND OF BINARY PSEUDO-RANDOM GRATING STANDARD

The BPR as we determine it here is a set of rectangular groves (of binary height levels) pseudo-randomly distributed over a uniform grid with an elementary pitch equal to the width of a groove. The term 'pseudo-random' depicts that the distribution is specially generated to possess a property of randomness in the mathematically strong sense.

*vvyashchuk@lbl.gov; phone 1 510 495-2592; fax 1 510 486-7696; www.lbl.gov

As it is shown below, the inherent PSD spectrum of such a grid is independent of spatial frequency (white-noise-like). Therefore, any deviation of a PSD spectrum measured with a real instrument from a white-noise-like spectrum would be a measure of the instrumental MTF.

The BPR grating-based method proposed here is in some sense an extension of the approach based on a unit step surface.[9-11] The inherent 1D PSD spectrum of a step artifact has an inverse-quadratic dependence on spatial frequency.[1] Such behavior of the step surface PSD puts a limitation on its use at higher spatial frequencies. The advantage of the proposed BPR grating, which comes from the spatial frequency independence of its PSD spectrum, is that it basically provides a uniform sensitivity to measurement of the MTF function at all desired frequencies. It also provides a measure of the system MTF averaged over the entire linear extent of the field of view, rather than just in a very localized region around the height discontinuity of the single step artifact.

Particular methods for generation of maximum-length pseudorandom sequences[12-14] were developed in connection with the use of pseudorandom chopping of a beam in time-of-flight experiments.[15-17] The sequences are mathematically represented with 1's, which denote an open chopper slot, and 0's, which denote a closed chopper slot. The chopping associated with a cross-correlation analysis of the measured time-resolved detector signal is favored over single-shot (periodic) chopping with the duty-cycle gain factor as high as $N/4$ (assuming two slits on a periodic chopper), where N is the length of the pseudorandom sequence.

Similar to the requirement for maximum duty cycle of a pseudorandom chopper, the BPR grating has to be generated with a maximum filling factor for an improved signal-to-noise ratio of the PSD spectra of the test surface. The mathematical term for such a sequence is "maximum-length pseudorandom sequence" (MLPRS).[13] Note that such sequences used for chopping are not entirely random, repeating themselves after N elements.

The analytical method we used to generate a MLPRS (modulo-two) of odd length $N = 2^n - 1$, where n is an integer, is described in.[13] In this article, all base ten values for the recursion coefficients (RC) which can be used for the generation of MLPRS are presented and the use of a particular RC to generate a pseudorandom sequence is explained.

A sequence $\{a_i\}$ of N elements ($i = 0, 1, \cdots, N-1$) to be qualified as a MLPRS must obey two conditions on its correlation function. First, the autocorrelation of the sequence must sum to 2^{n-1}. That means that the sequence's correlation function, which is determined as

$$A_j = \sum_{i=0}^{N-1} a_i a_{i+j}, \quad j = 0, 1, \cdots, N-1,$$

(1)

sums to $A_0 = 2^{n-1}$ (equal to the number of 1's in the MLPRS) at $j = 0$. Second, the sequence has to be 'almost' uncorrelated, which means that the cross-correlation of the sequence, A_j at $j \neq 0$ all are equal to each other, $A_j = 2^{n-2}$.[13] The conditions are very natural if one uses a definition of a purely random sequence (or process), or white noise, as a sequence which consists entirely of uncorrelated binary elements (impulses).[18]

Note here, that in order to construct a 'true' δ-function-like correlation function [that is $\delta(j \neq 0) = 0$ and $\delta(j = 0) = 1$] for a particular MLPRS, one can use a specially designed 'deconvolution' sequence (see e.g., Ref.[16])

$$b_i = \frac{2a_i - 1}{2^{n-1}}.$$

(2)

Then the expression analogous to Eq. (1) gives the δ-function-like correlation function

$$\Delta_j = \sum_{i=0}^{N-1} a_i b_{i+j} = \frac{1}{2^{n-2}} \sum_{i=0}^{N-1} a_i a_{i+j} - 1.$$

(3)

According to Eq. (3) $\Delta_0 = 1$ at $j = 0$ and $\Delta_j = 0$ at $j \neq 0$.

Based on the procedure described in Ref.[13], we generate a BPR sequence of $N = 4095$ elements obtained (see Ref.[13], Table III) with sequence generator $n = 12$ and the recursion coefficient $M = 83$ (base 10 value). Figure 1 graphically reproduces the first 100 elements of the BPR sequence.
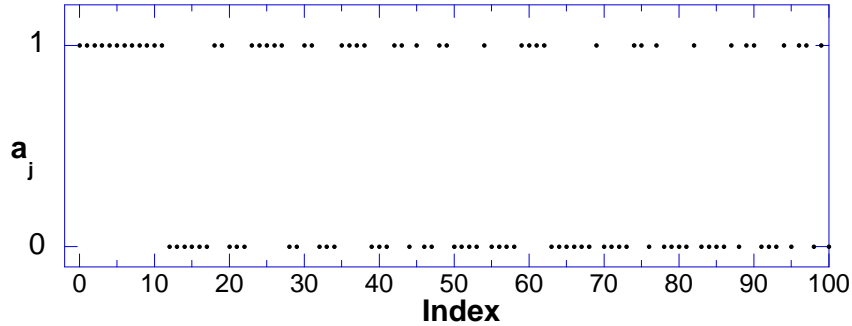

Figure 1: First 100 elements of the BPR sequence (see text for details).

3. PROTOTYPE OF BINARY PSEUDO-RANDOM GRATING STANDARD

A grating according to the generated BPR sequence was fabricated using a conventional lithographical process. The grating was etched into a silicon substrate. The fundamental feature width of the grating is 2.5 µm. The etch depth was measured with a calibrated atomic force microscope to be approximately 700 nm. However, the effective depth of the grating as it is seen by the Micromap™-570 interferometric microscope is only 174 nm. The discrepancy is due to the uncertainty of 2π of the phase-retrieval algorithm of the instrument. The uncertainty leads to the effective depth of the grating smaller by the wavelength of the light that is $\lambda = 520$ nm. Nevertheless, this circumstance does not compromise the possibility to calibrate the instrument with a standard with depth larger than λ, if the 2π phase shift due to the retrieval is applied to the entire surface measured. Moreover, with such a grating, one can test the capability of the instrument to reliably measure surface structures with concavities deeper than the wavelength of light.

Measurements made near the left (low index number) edge of the grating with the Micromap™-570 interferometric microscope using the 50x objective are shown in Fig. 2, along with the corresponding points of the ideal BPR grating pattern scaled to the 2.5 µm grid pitch.
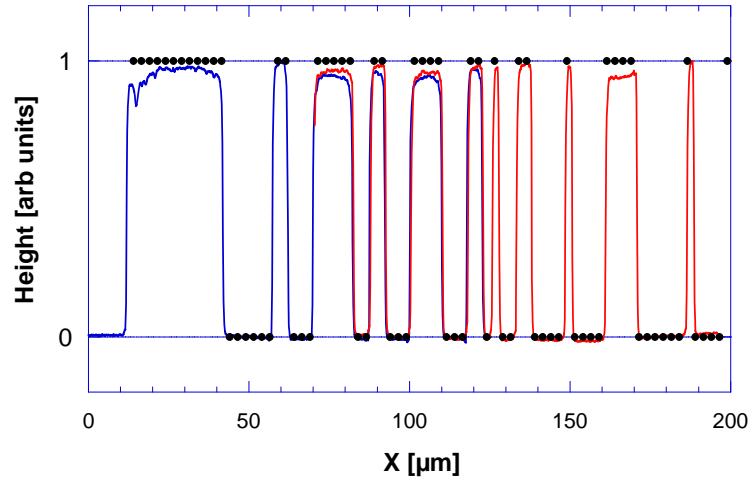

Figure 2: Measured profiles made near the left edge of a prototype BPR grating with a Micromap™-570 interferometric microscope with a 50x objective. Also shown are the corresponding points in the computed BPR function. The measured profiles are inverted to match the polarity of the computed function.

The field of view on the surface at this magnification for the profile measurement is about 125 µm, which corresponds to 50 feature elements on the grating. The starting points for the two measured profiles are shifted by about 70 µm, which corresponds to 28 grating elements. The measured profiles are inverted to match the polarity of the BPR sequence. One can see that the etching process leaves some residual roughness at the bottom of a groove (at the top of the plotted features in Fig. 2), since it is not yet optimized to produce the desired height and minimum residual roughness. However, since the deviations from the ideal profile are significantly smaller than the grating groove height, there should not be a noticeable perturbation of the resulting PSD spectrum of the grating. Moreover, a reasonable assumption about the random character of the perturbations suggests a white-noise-like spectrum of the perturbation that is the desired property of the BPRG test surface.

Figure 3 compares the 1D PSD spectrum of a unit-height 4095-element constructed BPR pattern with an element grid spacing of 1 µm computed over the entire 4095 point set (dashed straight line) with the PSD computed from subsets of the full 4095 element array. The noisy spectrum resulting when only the first 480 points are used in the calculation is shown as the red curve. The speckle noise is significantly reduced by averaging the spectrum of nine 480-point subsets of the main pattern, each shifted successively by 400 pixels. This latter curve corresponds more closely to the general observed case when the grating is viewed by a real microscope system. For the simulation, we use the same discrete PSD algorithm as the one described in Refs.[2-4]. The spectrum of the ideal BPRG function is indeed a white-noise-like straight line with no fluctuations and with an amplitude of 0.5. The amplitude corresponds to an expectation value based on the duty cycle of approximately 0.5 of the maximum-length pseudorandom sequence used in the construction.
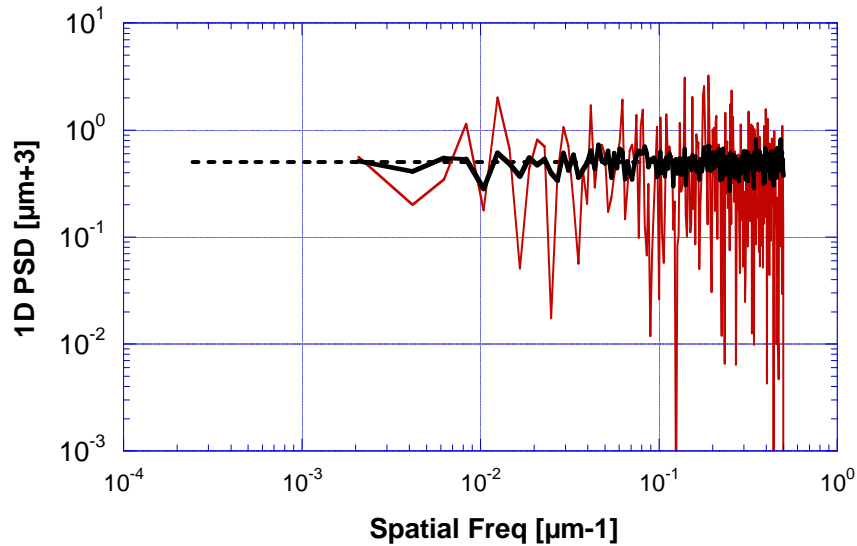

Figure 3: 1D PSD spectrum of the ideal unit-height BPR grating function with 4095 total number of pixels placed on a 1µm pitch grid: black (dashed) straight line includes all 4095 points in the calculation; red (solid) irregular line is from a subset of the first 480 points; black (solid) line is average of 9 480-point spectra, each shifted by 400 pixels.

For real experimental arrangements, when an instrument with finite detector pixel size is used, one can not expect the spacing of the grating projected onto the detector to line up exactly with the boundaries of each detector pixel. We simulated such a situation corresponding to a measurement with the Micromap[TM]-570 microscope with a 2.5x objective. The total number of detector pixels is 480 and the size of each pixel projected onto the grating is 3.92 µm. In this case, the grating pattern is undersampled and the pixel width encompasses more than one grating element. The simulation was aligned to have the first grating element at the left edge of the profile. The result of the simulation is shown in Fig. 4 together with the BPRG profile measured with the instrument over the same profile length. The corresponding PSD spectra are shown in Fig. 5.

The spectra in Fig. 5 are almost identical. That is the result of the deterministic character of the grating profile. The difference, seen for a few points at the lower spatial frequencies, is a result of the detrending with a two-dimensional second-order polynomial subtracted from the measured surface profile.
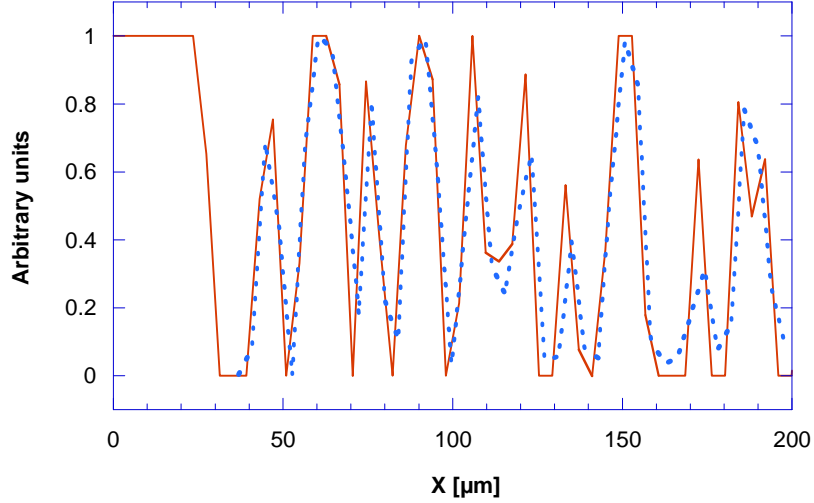
Figure 4: Profile of the first 200 μm of the 4095 element BPR grating with 2.5μm pitch: ideal computed function resampled to the 3.92 μm grid (red solid curve), and profile measured with the Micromap[TM]-570 microscope with 2.5x objective, (blue dashed curve).
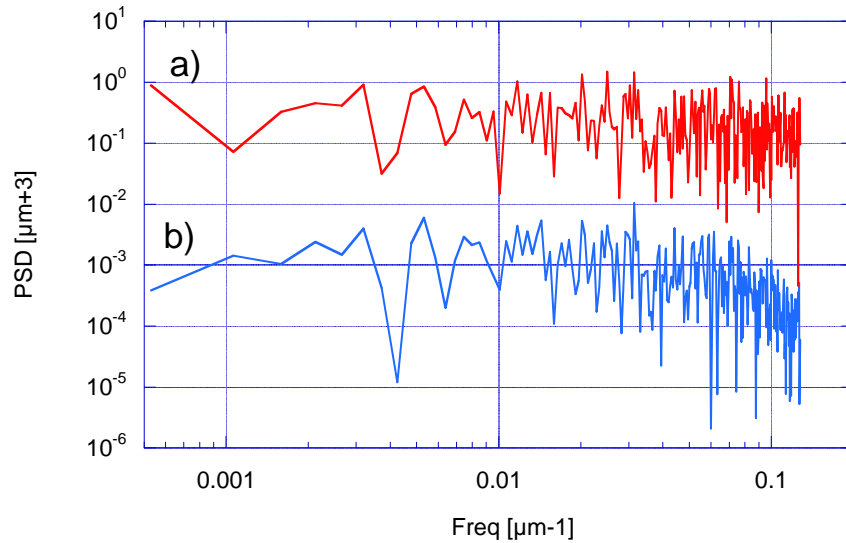

Figure 5: 1D PSD spectrum of the 4095 element, 2.5-μm pitch, BPR grating: a) (red, upper) for the model simulation resampled onto a 3.92μm grid, and b) (blue, lower) for the profile measured with the Micromap[TM]-570 microscope with 2.5x objective. The simulation and measurement fields of view correspond to the 480 pixel row length in the Micromap. Vertical offset of the lower spectrum is made for clarity.

4. MTF CORRECTION OF MICROMAP[TM]-570

The high frequency roll-off of the measured spectrum (Fig. 5b) is due in part to the instrumental MTF associated with sampling with finite pixels (see, e.g., Ref.[19]). This effect can be accounted with a Sinc-function-like MTF (see Ref.[2])

$$MTF_P(f_x, f_y) = \left(\frac{Sin\, \pi D_x f_x}{\pi D_x f_x} \right) \left(\frac{Sin\, \pi D_y f_y}{\pi D_y f_y} \right),$$ (4)

where f_x and f_y are the components of the spatial frequency, and D_x and D_y are the effective pixel sizes projected on to the surface plane. The result of application of the MTF (4) with an optimal effective size of a pixel of ~5.1 μm to the theoretical PSD spectrum (Fig. 5a) is shown in Fig. 6a. A figure of merit for the optimal correction was a coincidence of the measured BPRG PSD spectrum and the PSD inherent for the BPRG test surface corrected with the MTF (4). The effective size of a pixel (that is approximately 1.35 of size of a pixel of the Micromap[TM]-570 camera) found here with the BPR grating, coincides with the result of indirect calibration of the same instrument described in Refs.[2-4] Note that for PSD correction one should use the MTF function squared.

Even better correction can be achieved (Fig. 5b) by additionally adding an incoherent transfer function of a diffraction-limited objective in the form[19,20]

$$MTF_O(f) = \frac{2}{\pi}\left[-\Omega\sqrt{1-\Omega^2} + ArcCos\,\Omega \right],$$ (5)

where $\Omega = \lambda f / 2NA$, λ is the measuring wavelength (0.52 μm), $f = \sqrt{f_x^2 + f_y^2}$, and NA is the numerical aperture (0.075 for a 2.5x objective). After the correction, the measured and inherent PSD spectra of the BPRG are almost identical.

Figure 7 illustrate the efficiency of the MTF correction applied to the 1D PSD spectrum of the prototype BPRG measured with the Micromap[TM]-570 microscope with 2.5x objective. After correction for the lens MTF, the high frequency tail of the initial spectrum (Fig. 7a) is raised (Fig. 6b) but it is still exhibits significant roll off. The result of applying this correction with an optimal effective pixel size of 5.1 μm to the lens-corrected PSD is shown in Fig. 6c. In this case, the corrected PSD flattens out to a noisy horizontal line, becoming a white-noise-like spectrum, indicating that the applied MTF corrections are sufficient to account for the observed high-frequency roll-off.
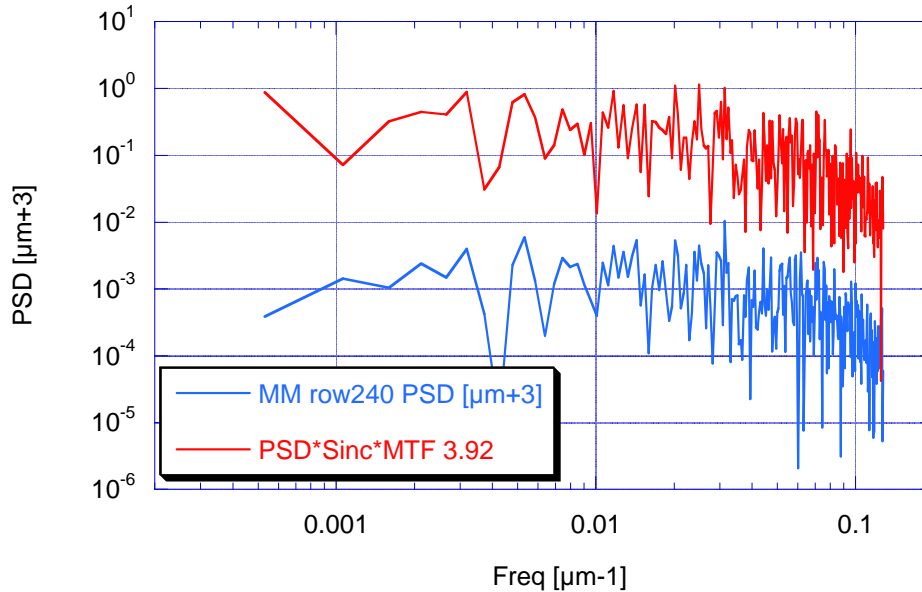

Figure 6: 1D PSD spectra of the BPRG with 4095 total number of elements with 2.5-μm pitch. The red colored spectrum corresponds to the theoretical BPRG PSD shown in Fig. 5a but corrected to account MTF due to the effective pixel size (4) and additionally corrected for the MTF of diffraction limited objective (5). The blue line depicts the PSD spectrum of the BPR grating standard described in the text. The experimental spectrum was measured with the Micromap[TM]-570 microscope with 2.5x objective. Vertical offset of the lower spectrum is made for clarity.
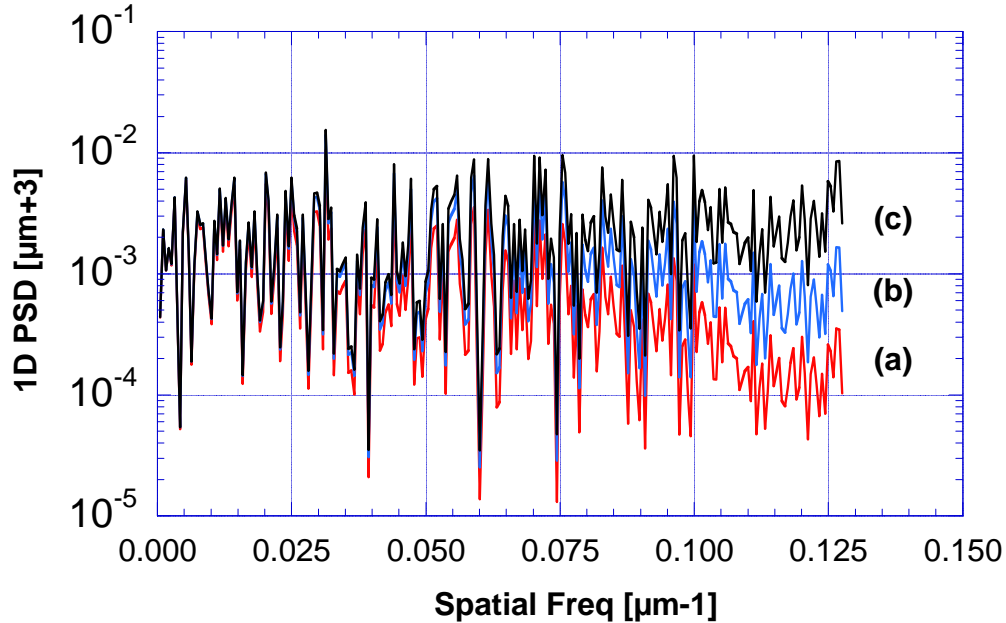
Figure 7: 1D PSD spectrum of the prototype BPRG with 4095 total number of elements with 2.5-μm pitch measured with the Micromap[TM]-570 microscope with 2.5x objective: a) (lower, red) average uncorrected raw PSD curve; b) (middle, blue) corrected to account for MTF due to the objective lens aperture, and c) additionally corrected for the MTF of the finite pixel width.

5. DISCUSSION AND CONCLUSION

Therefore, using the BPRG we are able to experimentally find the instrumental MTF and correct the measured PSD spectra for the MTF. The success of the correction is ensured by the deterministic character of the pseudorandom sequence used to fabricate the BPRG test surface and, therefore, the possibility to precisely simulate the PSD spectrum inherent for a certain part of the grating.

The choice of a binary pseudo-random sequence for the test grating has two major advantages compared with random 1D surfaces based on sequences obtained with random number generators or white noise sources. Both the advantages relate to the requirement of ease of specification and reproducibility of the test surface when used as a certified standard. *First*, a binary height distribution with two normalized heights, '1' and '0', can be easily specified for a number of production processes, e.g., lithography. The absolute value of the height would be determined based on requirements for a particular application, such as the range of measurable heights of the instruments. Possible perturbations of the shape of the rectangular grooves of a BPR grating would just lead to a slight change of overall amplitude of the flat PSD spectrum without any noticeable perturbation of its flat spatial frequency dependence for frequencies lower than the frequency corresponding to the characteristic size of a unit groove. *Second*, a pseudorandom sequence has spectral characteristics that are mathematically rigorous, reproducible and amenable to simulation, allowing one to *deterministically* construct a maximum-length random sequence with an ideal ('one-bit' wide) autocorrelation function optimal for a particular instrument.

As mentioned above, a distinguishing property of the BPR grating is that its PSD spectrum is a result of the distribution of the grooves, rather than the groove shape. This determines a low sensitivity of the BPRG PSD spectrum to the shape perturbation of a groove, which would be seen only at frequencies significantly higher than the Nyquist frequency of the instrument. In any case, if the perturbation is random, it does not change the inherent random (white-noise-like) character of the BPRG PSD spectrum. Moreover, the overall magnitude of the BPRG PSD spectrum is determined by the depth of the grooves. Therefore, for a reasonably designed BPRG standard, the contribution of the roughness of the grating surface can be easily made to be insignificant.

The deterministic character of the BPR grating allows precise simulation of the theoretical (ideal) PSD spectrum of the standard and comparison of it with an experimentally measured spectrum. But for some applications, the theoretical spectrum can be approximated with an ideal (without variation) white-noise-like spectrum. In this case, the amplitude of fluctuations of the measured PSD spectrum can be significantly decreased by averaging the PSD spectra measured at random shifts of the BPR grating with respect to the field of view of the instrument (compare with Fig. 3). A further reduction in the variance can be obtained if one applies an averaging procedure used in Ref.[13] In this case the measured height profiles are divided into a number of shorter length profiles and the PSD spectra of each subset are averaged.

Even though in this work we only discuss in detail the design and properties of a 1D BPR grating, the suggested approach can be easily extended to the two-dimensional (2D) case, if a test surface with a binary pseudo-random 2D pattern[21,22] were to be designed. Such a test surface would have the same advantages (a mathematically deterministic character and ease of specification and reproduction), mentioned above compared to a 2D gray random target generated with a generator of random numbers.[23] An additional advantage of the 2D pseudo-random PSD standard would be the possibility for a direct 2D calibration of the instrumental MTF. We also point out that the suggested calibration method using a BPR grating and/or the extended method based on a 2D pseudo-random test surface meets the requirements of ease of specification and reproducibility of a test surface used as a certified standard. Such investigations are in progress at LBNL and BNL.

ACKNOWLEDGMENTS

DISCLAIMER

Certain commercial equipment, instruments, software, or materials are identified in this document. Such identification does not imply recommendation or endorsement by the US Department of Energy, LBNL, BNL or the ALS nor does it imply that the products identified are necessarily the best available for the purpose.

REFERENCES

1. R. N. Bracewell, *The Fourier Transform and Its Applications* (McGraw-Hill Publishing Company, New York, 1986).
2. V. V. Yashchuk, A. D. Franck, S. C. Irick, M. R. Howells, A. A. MacDowell, W. R. McKinney, *Two dimensional power spectral density measurements of x-ray optics with the Micromap interferometric microscope*, SPIE Proceedings 5858, pp. 58580A-1-12.
3. V. V. Yashchuk, S. C. Irick, E. M. Gullikson, M. R. Howells, A. A. MacDowell, W. R. McKinney, F. Salmassi, T. Warwick, *Cross-check of different techniques for two dimensional power spectral density measurements of x-ray optics,* SPIE Proceedings 55921, pp. 59210G-1-12.
4. V. V. Yashchuk, E. M. Gullikson, M. R. Howells, S. C. Irick, A. A. MacDowell, W. R. McKinney, F. Salmassi, T. Warwick, J. P. Metz, T. W. Tonnessen, *Surface roughness of stainless-steel mirrors for focusing soft x rays*, Applied Optics 45(20), 4833-4842 (2006).
5. L. Assoufid, O. Hignette, M. Howells, S. Irick, H. Lammert, P. Takacs, *Future metrology needs for synchrotron radiation grazing-incidence optics,* Nucl. Instrum. and Meth. in Phys. Research A 467-468, 267-70 (2001).
6. E. L. Church, H. A. Jenkinson, and J. M. Zavada, *Relationship between surface scattering and microtopographic features,* Optical Engineering 18(2), 125-136 (1979).
7. D. Attwood, *Soft X-rays and Extreme Ultraviolet Radiation* (Cambridge University Press, New York, 1999).
8. G. D. Boreman, *Modulation Transfer Function in Optical and Electro-optical Systems* (SPIE Press, 2001).

9. K. Creath, *Calibration of Numerical aperture effects in interferometric microscope objectives,* Applied Optics 28(15), 3333-3338 (1989).

10. P. Z. Takacs, M. X. Li, K. Furenlid, E. L. Church, *Step-height standard for surface-profiler calibration*, SPIE Proceedings 1995, 235-44 (1993).

11. C. R. Wolfe, J. D. Downie, and J. K. Lawson, *Measuring the spatial frequency transfer function of phase-measuring interferometers for laser optics*, Proceedings of SPIE 2870 (1996), 553-7.

12. T. Etzon, *Construction for perfect maps and pseudorandom arrays,* IEEE Trans. on Information Theory 34(5), 1308-1316 (1988).

13. D. D. Koleske, and S. J. Sibener, *Generation of pseudorandom sequence for use in cross-correlation modulation,* Rev. Sci. Instrum. 63(8), 3852-3855 (1992).

14. H. D. Luke and A. Busboom, *Binary arrays with perfect odd-periodic autocorrelation,* Applied Optics 36(26), 6612-6619 (1999).

15. V. L. Hirschy, and J. P. Aldridge, *A Cross Correlation Chopper for Molecular Beam Modulation,* Rev. Sci. Instrum. 42(3), 381-383 (1971).

16. G. Comsa, R. David, and B. J. Schumacher, *Magnetically suspended cross-correlation chopper in molecular beam-surface experiments,* Rev. Sci. Instrum. 52(6), 789-791 (1981).

17. V. V. Yashchuk, B. N. Ashkinadzi, M. N. Groshev, V. F. Ezhov, T. A. Isaev, V. A. Knyazkov, G. B. Krygin, V. L. Ryabov, *Cross-Correlation Time-of-Flight Spectrometer of Gas-Dynamic Molecular Beams,* Instruments and Experimental Techniques, 40(4), 501 (1997).

18. G. M. Jenkins and D. G. Watts, *Spectral Analysis and its Applications*, fifth printing (Emerson-Adams Press, Boca Raton, 2000).

19. J. W. Goodman, *Introduction to Fourier Optics,* third edition (Roberts & Company Publishers, Englewood, 2005).

20. E. L. Church, P. Z. Takacs, *Effects of optical transfer function in surface-profile measurements*, Proceedings of SPIE, 1164 (1989), 46-59.

21. E. E. Fenimore, T. M. Cannon, *Coded aperture imaging with uniformly redundant arrays,* Applied Optics 17(3), 337-347 (2978).

22. E. Caroli, J. B. Stephen, G. Di Cocco, L. Natalucci, A. Spizzichino, *Coded aperture imaging in x- and gamma-ray astronomy,* Space Science Reviews 45, 349-403 (1987).

23. E. Levy, D. Peles, M. Opher-Lipson, and S. G. Lipson, *Modulation transfer function of a lens measured with a random target method,* Applied Optics 38(4), 679-683 (1999).